Ocean Engineering 296 (2024) 117097

Contents lists available at ScienceDirect

Ocean Engineering

journal homepage: www.elsevier.com/locate/oceaneng

Roll characteristics of the Naples Systematic Series

Fabio De Luca, Riccardo Pigazzini *, Gennaro Rosano, Tommaso Coppola

University of Naples Federico II, Department of Industrial Engineering, Via Claudio, 21, Naples, 80125, Italy

ARTICLE INFO

Keywords:
NSS systematic series
Planing hulls
Roll decay tests
Regular beam waves
Irregular beam waves

ABSTRACT

In the present paper, the results from an experimental campaign aimed at the characterization of the roll characteristics of the warped hard chine models of the Naples Systematic Series (NSS) are presented.

The Levenberg–Marquardt non-linear parameter identification technique has been employed to determine the damping and restoring coefficients from roll decay tests. Three differential models have been analysed to evaluate the one that provides the best fit of the experimental data. It is found a that quadratic damping model is sufficiently accurate to describe damping non-linearity, whereas a cubic restoring term is recommended to properly model the roll dynamics. Roll decay tests have been further analysed considering the linear decrement of the roll angle. The equivalent damping coefficient has been calculated for all the considered methods.

Response Amplitude Operators (RAO) in regular beam waves at zero speed are presented as well as roll-heave phase response. RAOs have shown a relatively similar response of the vessels in terms of roll and heave motions. Finally, an analysis of the behaviour of the hard chine hull forms in irregular beam waves is presented, with particular emphasis on roll and heave amplitude and phase responses.

1. Introduction

The systematic experimental studies of the seakeeping of planing hull performances in rough water started in the late 60's with the studies carried out by Fridsma (1969, 1971). His work dealt with both calm water, regular and irregular wave data of a family of prismatic planing hulls. The work of Fridsma was extended by Zarnick and Turner (1981) by using longer hull models in order to assess the effect of L/B ratio on the seakeeping performances. The results showed poor seakeeping abilities of the prismatic hull respect to a conventional bow. More recently, Taunton et al. (2011) presented the seakeeping results of eight models in irregular head waves at three different speeds, Begovic et al. (2014) studied effect of hull warping on heave, pitch and vertical accelerations in regular and irregular waves (Begovic et al., 2016). The results showed that warped hullforms led to better seakeeping performances with respect to the prismatic hulls, particularly in terms of acceleration response.

In recent years, the Naples Systematic Series (NSS) (De Luca and Pensa, 2017) has been developed with the aim to have good seakeeping abilities through a warped hard chine hull with raising keel line towards the stern. In order to mitigate the loss in calm water efficiency, the parent hull has been designed taking into account the use of interceptors.

As the NSS has been thoroughly studied both for its calm water (De Luca and Pensa, 2017), regular (Pigazzini et al., 2021) and irregular (De Luca and Pensa, 2019) seakeeping performances, only motions in the longitudinal plane have been investigated.

In light of the experimental facilities limitations and the need to investigate the roll characteristics of the NSS hulls, a set of experiments at zero speed has been devised to estimate non-linear roll restoring and damping coefficients, as well as roll response in regular and irregular beam waves.

The main objective of the present paper is to further investigate the seakeeping characteristics of the Naples Systematic Series, which has been studied for longitudinal waves in previous research works, Pigazzini et al. (2021), and De Luca and Pensa (2019). The work focuses on the analysis of the roll characteristics of the NSS, based on the results from an experimental campaign conducted in the towing tank of the Università degli Studi di Napoli Federico II. In addition, the proposed results are intended to be a source of data for the investigation of roll motion behaviour of hard chine warped planing hulls, which, due to the peculiar geometry, have a different hydrodynamic behaviour compared to conventional hull forms and for which few data are publicly available.

Roll damping coefficients are derived based on roll decay tests, examined by the application of the Levenberg–Marquardt algorithm and according to the recommended procedure of the International Towing Tank Conference (ITTC). Roll and heave Response Amplitude Operators

* Corresponding author.
E-mail addresses: fabio.deluca@unina.it (F. De Luca), riccardovasco.pigazzini@unina.it (R. Pigazzini), gennaro.rosano@unina.it (G. Rosano), tommaso.coppola@unina.it (T. Coppola).

https://doi.org/10.1016/j.oceaneng.2024.117097
Received 13 November 2023; Received in revised form 2 February 2024; Accepted 8 February 2024
Available online 13 February 2024

Nomenclature

Symbol	Description
L_{OA}	Length Overall (m)
L_{WL}	Waterline Length (m)
B_{WL}	Waterline Breadth (m)
LCG	Longitudinal Center of Gravity (m)
VCG	Vertical Center of Gravity (m)
Δ	Model weight (kg)
T	Draught (m)
k_{44}	Roll radius of gyration (m)
k_{55}	Pitch radius of gyration (m)
ω_0	Natural roll frequency (rad/s)
μ	Linear damping coefficient (1/s)
μ_e	Equivalent linear damping coefficient (1/s)
β	Quadratic damping coefficient (1/rad)
δ	Cubic damping coefficient (s/rad^2)
λ	Wavelength (m)
H	Wave height (m)
Fr	Froude number ($v/\sqrt{gL_{WL}}$) (−)
k	Wave number (rad/m)
ζ_w	Wave amplitude (m)
ϕ	Roll angle (rad)
ϕ_m	Measured roll angle (rad)
ζ_g	Heave (m)

(RAO) at zero speed in beam waves are experimentally derived. Finally, results of roll and heave responses in irregular waves are shown and discussed.

In the case of planing hulls, sources of roll damping that are not present in conventional hull forms can be identified. Flow separation from the chine is the main part of the eddy making component while the horizontal lift component tends to be small at high speeds due to the limited lateral wetted area (ITTC, 2011). At planing regime, an additional source of damping is generated by the vertical component of the lift acting on the wetted surface, whose magnitude is affected by the running trim angle. Roll damping of a planing hull at high speed may be significantly underestimated if such a component is neglected. A method for the prediction of the lift force contribution to roll damping was presented in Ikeda and Katayama (2000), based on a quasi-static approach, to be added to the other components determined by the original Ikeda's method (Ikeda et al., 1978a,b). The method, suitable when experimental decay tests are not available, showed a good agreement between predicted and experimental results.

Differently from displacement hull forms, for which many experimental and numerical data regarding roll damping and roll response in beam waves can be found in the literature, only few data can be identified for planning vessels. Three unappended prismatic hull forms, having deadrize angle of 10, 20 and 30 degrees and constant length to beam ratio 5, typical of patrol boats operating in the 90's, were tested in Brown and Klosinski (1995a,b). For each model, roll decay tests were performed at three different speeds, on a range of trim and yaw angles, to determine the added mass in roll and the damping coefficient. Empirical formulas were provided, based on the regression of the experimental data.

The effect of the model speed on the roll behaviour of prismatic hull forms was experimentally investigated in Balsamo et al. (2001), in both semi-planing and planing regime. An external harmonic roll moment, generated by two counter-rotating masses, was applied to model, restrained to the towing carriage, at different frequencies.

Roll angle was measured for each test condition and used to find the hydrodynamics coefficients. It was shown that its amplitude increases with speed at low frequencies, while an opposite behaviour at high frequency. At low speed, the roll damping coefficient showed higher values at high frequency; at high speed, an opposite behaviour was identified. An expected increase of roll damping was observed with the increase of the ship speed.

Experimental roll decay tests for two hull forms, a round bilge hull form and a hard chine, were presented in Begovic et al. (2013), at different speeds, to investigate the effect on the roll damping coefficients of the presence of the chine on the aft part of the vessel. The models had the same dimensions, displacement, metacentric height and warped bottom hull form. The equivalent damping coefficients of the two hull forms resulted comparable at moderate speed; at higher speed the equivalent damping of the hard chine hull form resulted significantly larger than the one or the round-bilge hull form, thanks to higher vertical lift force and increased flow separation at the chine.

Nowadays, Computational Fluid Dynamics is a viable alternative thanks to its accuracy, although many applications focused on displacement or semi-displacement hull forms, as Mancini et al. (2018). The effect of forward speed, roll amplitude and oscillation frequency was numerically investigated in Kahramanoglu et al. (2021). Roll damping coefficients were calculated through forced roll simulations; the obtained results were compared with available experimental data. Simulations showed the major contribution to the roll damping at high speeds is given by the vertical lift force.

The present paper is organized as follows. The main characteristics of the studied hull forms and the experimental setup are presented in Section 2. Section 3 collects the main results from the analysis of the experiments, consisting of roll decay tests, and regular and irregular beam waves. Main conclusion are summarized in Section 4.

2. Experimental setup

In this study, the models C3, C4 and C5 of the Naples Systematic Series (NSS) (De Luca and Pensa, 2017) have been used. In Fig. 1 the body plan and buttock lines of the parent C1 model are shown. The models were tested in the towing tank of the Department of Industrial Engineering of the Università degli Studi di Napoli Federico II. The tank is 136.0 m in length, 9.0 m wide and 4.5 m deep.

Models were tested at zero speed ($Fr = 0$) and were not restrained to the towing carriage. The same mass configuration used in De Luca and Pensa (2019) has been adopted, see Table 1.

Roll characteristics of the three hulls were studied by roll decay tests and regular and irregular beam waves. Additionally, for the free decay test analysis, the data of two smaller hulls from the systematic series has been included (C1s and C2s, De Luca and Pensa, 2019; Pigazzini et al., 2021).

A unidirectional flap wavemaker was used to generate regular and irregular waves and their profile has been measured using AKAMINA AWP-24-2 Wave Height Gauges capacitive probes and Baumer UNDK 30U6103 ultrasonic probes. Active force feedback mode and specifically designed beach limited the wave reflection from the opposite side of the tank. A sub-millimeter precision optical motion tracking system, Qualisys Motion Capture System, fixed to the towing carriage has been used to capture the body motions.

3. Results and discussion

The knowledge of the roll motion characteristics of a ship is of paramount importance in assessing safety, operability and comfort. Mathematical models with different levels of complexity may be adopted to describe the roll motion. The accurate description of external excitation, together with hydrodynamic and restoring coefficients, is necessary to properly describe the roll behaviour of the ship and evaluate seakeeping performances. In the following subsections experimental results from decay tests, regular and irregular beam waves performed on the models of the NSS are presented and discussed.

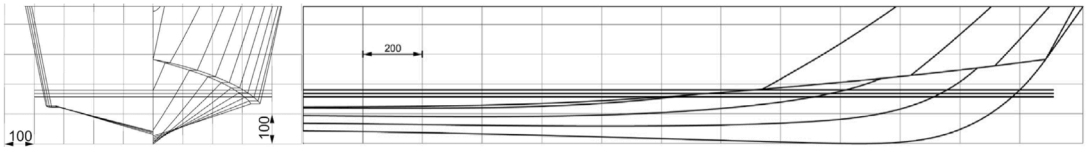

Fig. 1. C1 Model body plan and profile.

Table 1
Hulls specifications.

Model	C1s	C2s	C3	C4	C5
L_{OA} (m)	1.567	1.567	2.611	2.611	2.611
L_{WL} (m)	1.440	1.440	2.400	2.400	2.400
B_{WL} (m)	0.446	0.396	0.576	0.493	0.410
L_{WL}/B_{WL}	3.23	3.64	4.17	4.87	5.85
B_{WL}/T	4.12	4.12	4.12	4.12	4.12
LCG (m)	0.567	0.567	0.945	0.945	0.945
VCG/B_{WL}	0.50	0.50	0.50	0.50	0.50
Δ (kg)	26.52	20.91	73.93	54.12	37.40
k_{44}/B_{WL}	0.400	0.400	0.400	0.402	0.403
k_{55}/L_{WL}	0.250	0.250	0.251	0.250	0.253

3.1. Roll decay tests

A series of roll decay tests has been carried out by locating the models at the towing tank midpoint with the model's longitudinal axis perpendicular to the tank longitudinal axis, to avoid wave reflections from the towing tank sides. The rolling motion has been initialized by heeling the model by hand and releasing it. Each free decay time series has been trimmed at the first zero crossing before performing the parameter identification to exclude any disturbances due to the release procedure.

The free roll decay in still water can be described by a one degree of freedom (DOF) motion model, through a homogeneous second order differential equation, with non linear damping and restoring terms, which details can be found in (Bulian et al., 2009):

$$\ddot{\phi} + d(\dot{\phi}) + \omega_0^2 \cdot r(\phi) = 0 \tag{1}$$

where: ω_0^2 is the natural roll frequency; $d(\dot{\phi})$ and $r(\phi)$ describe non-linearity in damping and restoring. Typically, the damping term is expressed by a quadratic or a cubic function of the roll velocity:

$$d(\dot{\phi}) = 2\mu\dot{\phi} + \beta\dot{\phi}|\dot{\phi}| + \delta\dot{\phi}^3 \tag{2}$$

where μ, β and δ are the linear, quadratic and cubic damping coefficients, respectively.

A odd polynomial representation can be adopted for $r(\phi)$:

$$r(\phi) = \phi + \gamma\phi^3 + \cdots \tag{3}$$

where γ is the coefficient of the cubic term of the non-dimensional righting arm, Bulian et al. (2009).

In the following, a discussion on the order of the polynomials that provides the best description of the roll decay of the NSS models is provided. Additionally, two different methodologies are used and discussed to derive the coefficients of 1-DOF roll motion equation, namely a parameter identification technique (PIT) and the analysis of the linear decrement of roll decay, ITTC (2011).

The first analysed roll motion model considers a quadratic representation of damping and a cubic expression for restoring:

$$\ddot{\phi} + 2\mu\dot{\phi} + \beta\dot{\phi}|\dot{\phi}| + \omega_0^2\phi + \omega_0^2\gamma\phi^3 = 0 \tag{4}$$

with initial conditions:

$$\dot{\phi}(0) = \dot{\phi}_0, \;\; \phi(0) = \phi_0 \tag{5}$$

Alternatively, as suggested in ITTC (2011), the model for the roll angle can be described by the following differential equation, which adopts a cubic representation for the damping term and a linear one for restoring:

$$\ddot{\phi} + 2\mu\dot{\phi} + \beta\dot{\phi}|\dot{\phi}| + \delta\dot{\phi}^3 + \omega_0^2\phi = 0 \tag{6}$$

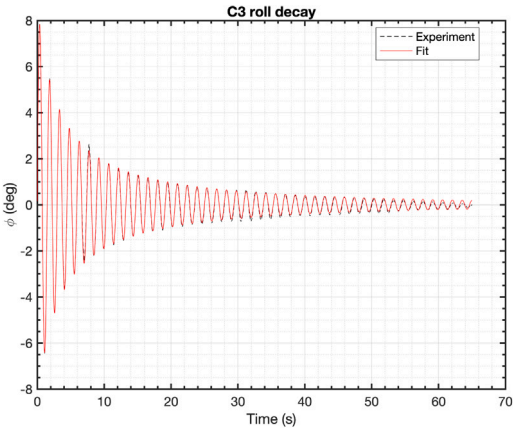

Fig. 2. Comparison of experimental and simulated (Eq. (4)) free decay data for C3 hull.

Given N_S samples of the roll angle in time $\phi(t_i)$, the set of constant μ, β, ω_0, γ or δ and initial conditions $\dot{\phi}_0, \phi_0$ that produces the best fit between the model in Eq. (4) and experimental results is found by minimizing the squares of the residuals χ^2:

$$\chi^2 = \sum_{i=0}^{N_S} \left[\phi_m(t_i) - \phi(t_i)\right]^2 \tag{7}$$

where ϕ_m is the measured roll angle at time t_i.

Preliminary, the Levenberg–Marquardt (Levenberg, 1944; Marquardt, 1963) algorithm has been employed in order to solve the non-linear least squares problem. The application of such an algorithm to characterize non-linearity of both damping and restoring, through the identification of a set of "optimum" parameters that minimizes χ^2, can be seen as a parameter identification technique, IMO (2006).

Given that Eq. (7) depends on the number of samples, which differs between the hull model tests, R^2 is used to evaluate the goodness of fit between different models:

$$R^2 = 1 - \frac{\chi^2}{\sum_{i=0}^{N_S}\left[\phi_m(t_i) - \phi(t_i)\right]^2} \tag{8}$$

In Fig. 2, the experimental roll angle time series from the experiment on the C3 hull is reported along with the solution of Eq. (4) using the fitted parameters obtained through the Levenberg–Marquardt algorithm, summarized in Table 2.

Looking at the results of the parameter identification for Eqs. (4) and (6), which are summarized in Tables 2 and 3, it can be seen that the model with a cubic restoring term shows a better fit (higher R^2) respect to the model with cubic damping term. That means that in the case of hard chine hullforms of the NSS, it is more important to consider the non-linearity in restoring than adding a third degree polynomial term to the damping. Nonetheless, both non-linear terms are nonzero.

Table 2
Parameter identification results for Eq. (4).

Model	μ	β	ω_0	γ	R^2
C1s	0.034153	0.660551	4.591486	−3.04659	0.997990
C2s	0.040403	0.800472	4.996607	−1.69338	0.996694
C3	0.020838	1.086905	4.279392	−2.06115	0.997412
C4	0.046807	0.986148	4.667468	−2.71886	0.997333
C5	0.106733	0.750320	5.146291	−2.95716	0.998260

Table 3
Parameter identification results for Eq. (6).

Model	μ	β	ω_0	δ	R^2
C1s	0.034282	0.679368	4.553320	0	0.990618
C2s	0.036524	0.849897	4.970156	0	0.988525
C3	0.023866	0.946766	4.273722	0.474923	0.995777
C4	0.052252	0.898518	4.638740	0.199382	0.994326
C5	0.125486	0.451888	5.110097	0.531780	0.995981

Table 4
Parameter identification results for Eq. (9).

Model	μ	β	ω_0	γ	δ	R^2
C1s	0.036616	0.637384	4.593515	−3.216677	0	0.997961
C2s	0.045377	0.747654	4.998303	−1.907032	0	0.996419
C3	0.023292	0.986605	4.279404	−2.057520	0.284810	0.997439
C4	0.046807	0.986148	4.667467	−2.718842	0	0.997333
C5	0.119946	0.555960	5.146168	−2.948325	0.274413	0.998271

A combination of Eqs. (4) and (6), where both non-linear damping and restoring terms are present, is also considered, as it could result in a better suited model for the free decay:

$$\ddot{\phi} + 2\mu\dot{\phi} + \beta\dot{\phi}|\dot{\phi}| + \delta\dot{\phi}^3 + \omega_0^2\phi + \omega_0^2\gamma\phi^3 = 0 \tag{9}$$

The results of the parameter identification for Eq. (9), provided in Table 4, show that for the C3 and C5 hulls the model with third order damping and restoring terms provides only a marginally better fit to the experimental data. The parameter identification for the other hulls shows that the best fit is found without third order damping term, i.e. Eq. (4). It is however clear that the simpler model Eq. (4) can provide a fit with comparable R^2 values to the more complex model given by Eq. (9).

In general, it is observed that the differential model of Eq. (4) with a cubic restoring provide a good fit to experimental data, with values of $1 - R^2$ of the order of 10^{-3}. The addition of a further non-linear damping term provides a negligible improvement.

As expected, the coefficient γ of the cubic restoring parameter is always negative, since the relation of the righting arm $\overline{GZ}(\phi)$ is best modelled as a softening spring.

The roll natural angular frequency ω_0 is also increasing as the slenderness increases, that could be counter intuitive as the initial stability is decreasing due to the diminishing waterplane transverse moment of inertia. However, the transverse mass moment of inertia is also decreasing leading to the identified increase of the natural roll frequency.

As an alternative to the PIT, the calculation of the damping coefficients has been also performed via analysis of the linear decrement of roll decay, the recommended procedure suggested in ITTC (2011), assuming Eq. (6) as reference model. In analysing Eq. (6) both a quadratic and a cubic representation of damping have been assumed, whose results are summarized in Table 5. It can be observed that the adopted procedure returns smaller R^2 values compared to derivation of the same coefficients by the Levenberg–Marquardt, for the same motion model.

Finally, the introduction of an equivalent linear roll damping coefficient μ_e, is a common practice to overcome the inherent complexity of the non-linear representation of the roll motion, (ITTC, 2011):

$$2\mu_e\dot{\phi} = 2\mu\dot{\phi} + \beta\dot{\phi}|\dot{\phi}| + \delta\dot{\phi}^3 \tag{10}$$

Table 5
Damping coefficients and natural roll frequency according to ITTC (2011), Eq. (6). Results for both the quadratic and cubic representation of the non-linear damping.

Model	μ	β	ω_0	δ	R^2
C1s	0.032338	0.655320	4.566	0	0.963933
C1s	0.042584	0.541445	4.566	0.122057	0.963689
C2s	0.016390	0.923894	4.975	0	0.972061
C2s	0.058196	0.507068	4.975	0.149025	0.967268
C3	0.020563	1.078593	4.278	0	0.980310
C3	0.006673	1.362207	4.278	−0.553629	0.978578
C4	0.036307	1.057107	4.675	0	0.960859
C4	0.043748	0.953975	4.675	0.149025	0.961075
C5	0.090435	0.848693	5.119	0	0.989626
C5	0.148851	0.103132	5.119	0.952596	0.989874

Table 6
Equivalent linear roll damping coefficient.

Model	ω_0	μ	β	δ	$\mu_{e,5deg}$	
C1s	4.566	0.0323	0.6553	0	0.1432	ITTC
	4.566	0.0426	0.5414	0.1221	0.1414	ITTC
	4.591	0.0342	0.6606	0	0.1465	L-M, Eq. (4)
	4.553	0.0343	0.6794	0	0.1489	L-M Eq. (6)
	4.594	0.0366	0.6374	0	0.1451	L-M Eq. (9)
C2s	4.975	0.0164	0.9239	0	0.1866	ITTC
	4.975	0.0582	0.5071	0.3921	0.1793	ITTC
	4.997	0.0404	0.8005	0	0.1885	L-M, Eq. (4)
	4.970	0.0365	0.8499	0	0.1930	L-M Eq. (6)
	4.998	0.0454	0.7477	0	0.1838	L-M Eq. (9)
C1	3.537	0.0251	0.6553	0	0.1109	ITTC
	3.537	0.0330	0.5414	0.1576	0.1096	ITTC
	3.557	0.0265	0.6606	0	0.1135	L-M, Eq. (4)
	3.527	0.0266	0.6794	0	0.1153	L-M Eq. (6)
	3.559	0.0284	0.6374	0	0.1124	L-M Eq. (9)
C2	3.854	0.0127	0.9239	0	0.1446	ITTC
	3.854	0.0451	0.5071	0.5061	0.1389	ITTC
	3.871	0.0313	0.8005	0	0.1461	L-M, Eq. (4)
	3.850	0.0283	0.8499	0	0.1495	L-M Eq. (6)
	3.872	0.0352	0.7477	0	0.1424	L-M Eq. (9)
C3	4.278	0.0206	1.0786	0	0.1915	ITTC
	4.278	0.0067	1.3622	−0.5536	0.1936	ITTC
	4.279	0.0208	1.0869	0	0.1931	L-M, Eq. (4)
	4.274	0.0239	0.9468	0.4749	0.1985	L-M Eq. (6)
	4.279	0.0233	0.9866	0.2848	0.1946	L-M Eq. (9)
C4	4.675	0.0363	1.0571	0	0.2193	ITTC
	4.675	0.0437	0.9540	0.1490	0.2182	ITTC
	4.667	0.0468	0.9861	0	0.2173	L-M, Eq. (4)
	4.639	0.0523	0.8985	0.1994	0.2189	L-M, Eq. (6)
	4.667	0.0468	0.9861	0	0.2173	L-M, Eq. (9)
C5	5.119	0.0904	0.8487	0	0.2513	ITTC
	5.119	0.1489	0.1031	0.9526	0.2397	ITTC
	5.146	0.1067	0.7503	0	0.2497	L-M, Eq. (4)
	5.110	0.1255	0.4519	0.5318	0.2507	L-M, Eq. (6)
	5.146	0.1199	0.5560	0.2744	0.2467	L-M, Eq. (9)

Typically, the equivalent coefficient μ_e is defined for a given roll amplitude ϕ_a as follows:

$$\mu_e = \mu + \frac{4}{3\pi}\omega_0\phi_a\beta + \frac{3}{8}\omega_0^2\phi_a^2\delta \tag{11}$$

The equivalent linear damping coefficient has been calculated for the selected vessels, assuming 5 degrees as reference angle. The obtained results are summarized in Table 6 and graphically represented in Fig. 3, for all the considered mathematical models. In particular, the results for C1 and C2 models have been scaled from C1s and C2s, in order to compare the equivalent linear damping coefficients for all the models of the series at the same model scale. It can be observed that the obtained values at 5 degrees are relatively close to each other. A general increase of the damping can be identified with length over breadth ratio, i.e. the more slender is the model the higher is the equivalent linear damping, which can be partly due to the reduction of mass moment of inertia for the most slender model, i.e. model C5.

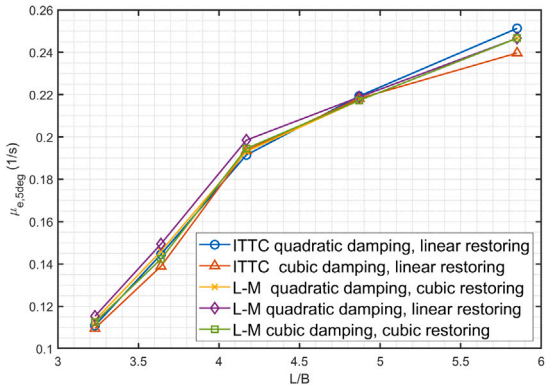

Fig. 3. Equivalent linear damping vs. L/B.

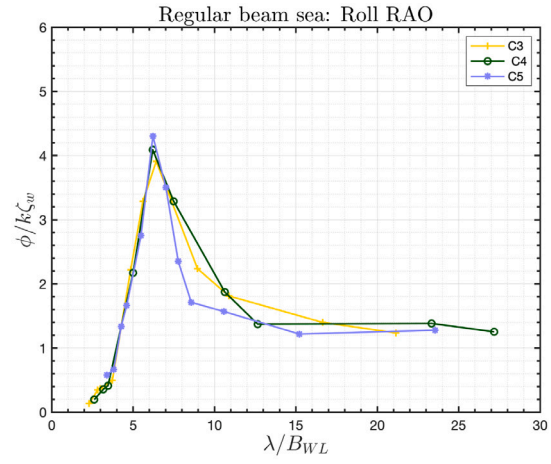

(a) Roll response comparison

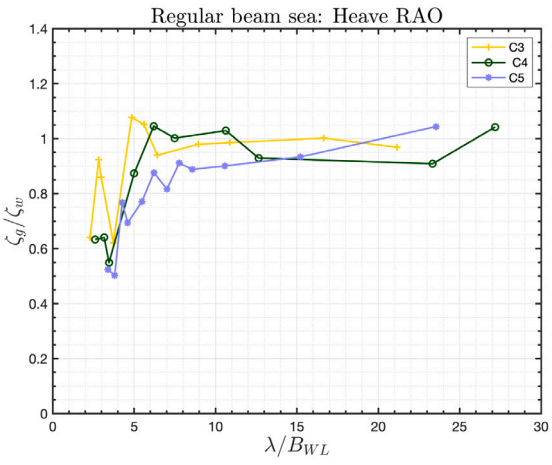

(b) Heave response comparison

Fig. 4. Comparison of hull motions RAOs.

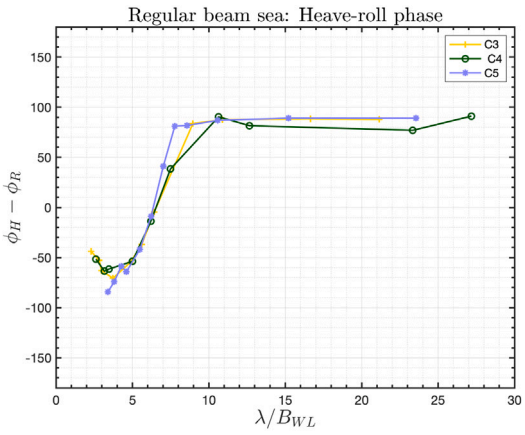

(a) Heave-roll phase response

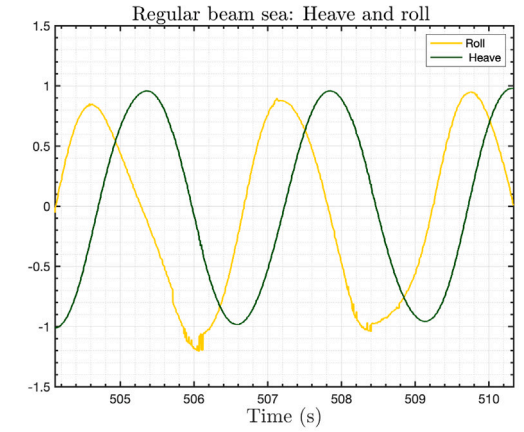

(b) Example of roll and heave time series

Fig. 5. Heave-roll phase.

3.2. Regular waves motion response

The regular waves seakeeping test program is comprised of a set of nine wavelengths with a target wave steepness of 1/50. The resulting wavelength to beam ratios spans between 2 and 27, corresponding to the range of wave angular frequencies from 2.0 to 7.3 rad/s. In the analysis of the beam sea response data, response amplitude operators (RAOs) have been computed using the ratio of the first harmonic amplitude of the response signal and the forcing term.

In Fig. 4(a), the comparison of the roll response of the three hulls is shown. It can be clearly seen that the hulls have almost the same wavelength to model breadth ratio for which roll is maximized. All the models show similar roll response from the shortest to the resonant wavelength. Differences are more evident for longer than resonant wavelength, until the roll RAOs tends to go towards unity for long waves, as expected.

The heave response plot in Fig. 4(b) shows no particular similarities between the three hulls apart the general trend towards longer waves. At the critical wavelengths for roll response, a slight decrease in heave response is observed as hull slenderness increases. This can be related to higher roll-heave coupling of the broader hull.

Since the hull was free to drift during the experiments, the wave profile measurement (fixed to the stationary carriage) is not relative to the actual position of the hull (due to drifting), and a direct phase assessment between wave and hull motion was not possible. Roll-heave phase has been instead evaluated using an FFT-based algorithm and results are plotted in Fig. 5. Roll-heave phase could nonetheless be considered as the roll phase respect to wave elevation, as heave-wave phase is essentially always zero for the wavelength to breadth ratios considered in this investigation.

In Fig. 5(a), the heave-roll phase response for the three hulls is plotted. As expected, it can be observed that phase is zero at the peak

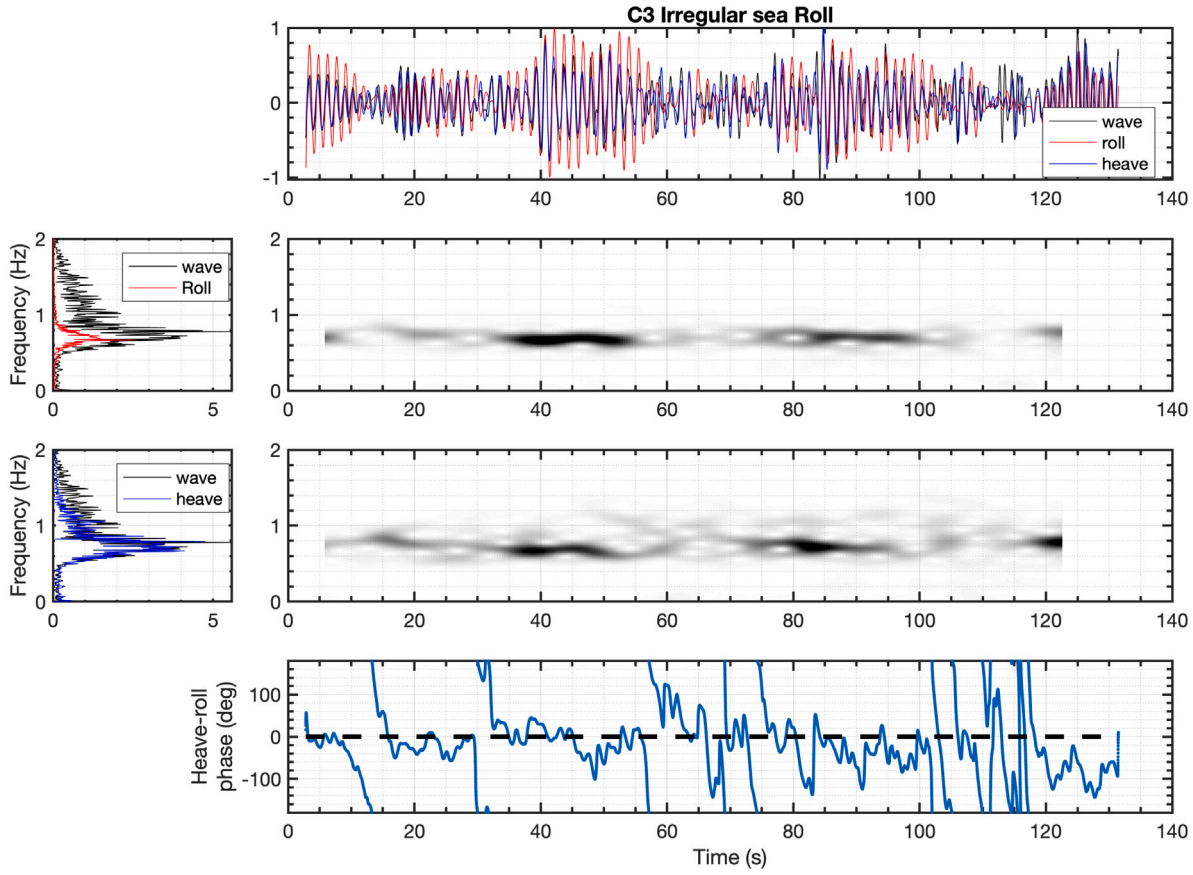

Fig. 6. C3 model irregular waves response.

of roll response, and for long waves roll motion leads heave by 90°, a sample of the timeseries for $\lambda/B_{WL} \approx 17$ is shown in Fig. 5(b). It can be observed that the transition from in phase to 90° roll is reached by the most slender hull at shorter wavelengths to beam ratios (steeper phase transition).

3.3. Irregular waves motion response

The results from irregular waves tests on the hulls are presented using both frequency domain and time-frequency analyses to investigate phase shifts and spectral contents of the motion response of the three hulls. The sea state used in this investigations is defined by the JONSWAP spectrum ($\gamma = 3.3$, $H_S = 0.060$ m, $T_P = 1.356$ s), as in De Luca and Pensa (2019).

Figs. 6, 7 and 8 on roll response show six subplots each. Starting from the top one, normalized wave elevation, roll and heave amplitude signals are plotted; the second row of plots shows the spectra of roll and wave signals on the first plot on the left, where the second plot show the spectrogram (b/w gradient) of the roll response signal computed using short-time Discrete Fourier Transform (STFT) (here the variable spectral content of the roll response signal is plotted against time); on the third row, the same subplots are presented for the heave motion. The bottom plot (blue line) instead shows the instantaneous phase of roll response with respect to the heave amplitude. The instantaneous phase delay is computed using a Hilbert transform-based algorithm.

As expected, heave response is much more related to wave elevation respect to the roll motion. Looking at the global spectra comparison plots (first plots of second and third row), there is a far better overlap between the wave and heave spectra, with respect to the wave roll spectra, for all three hulls.

For all three cases, even if the average spectral content of both heave and roll responses present a well defined peak, the same is not valid all the times. At times when the roll signal is characterized by a short time spectra with a single defined peak, the spectrogram shows a darker, uniform streak. The grey areas of the spectrogram shows when roll response is characterized temporarily by a broader bandwidth spectrum. Where this occurs, it is frequent to notice white spots (or circular grey contours). This indicates that at one time, the monochromatic roll motion (with a single predominant harmonic, around 75 s mark in Fig. 6) transitions to a dichromatic motion with frequencies that are close one to the other (beating). This is clearly visible in the top time history plot, where around the same timestamp, a beat in the roll signal can be observed (between 75 to 85 s mark), the frequency of the beating is roughly 0.1 Hz, as it is the diameter of the circle at the 80 s mark in the middle plot.

Looking at the bottom plot of Figs. 6–8, the instantaneous phase between heave and roll response shows that some constant phase periods (monochromatic response, darker, single streaks in the second and third row plots) are separated by phase transitions. Where the phase difference seems to be more stationary, the average value is around 0° (heave and roll in phase). The average peak response frequency (and sea modal frequency) is around 0.8 Hz, that translates to a value of $\lambda/B_{WL} \approx 6$. Looking at the plot in Fig. 5(b), the phase response for $\lambda/B_{WL} \approx 6$ is indeed around 0 degrees.

It can be noted also that as the roll amplitude increases both its spectra and phase are better defined. Since the phase between two signals is only defined if both are monochromatic, the phase transition

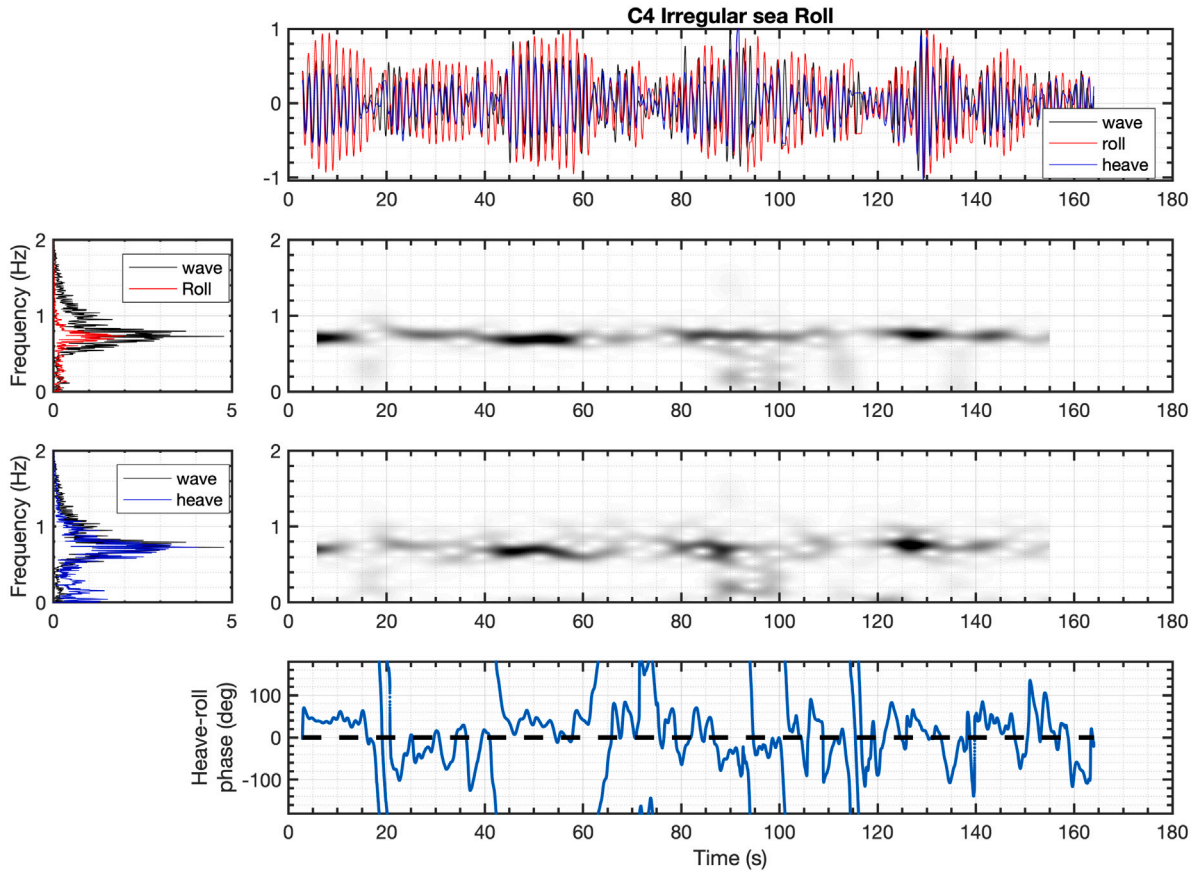

Fig. 7. C4 model irregular waves response.

periods are to be ascribed to the multi-chromatic nature of roll and/or wave elevation signals. In other words, there are no rapid shifts in phase (around 100–120 s mark in Fig. 6), but instead the phase between roll and wave signals cannot be defined in those time intervals.

4. Conclusions

The present paper presents the results of an experimental evaluation of the roll characteristics of the Naples Systematic Series hard chine models. The characterization of the damping and restoring coefficients of the non-linear differential equations that may be used to model the free roll decay, as well as the analysis of roll and heave response in regular and irregular beam sea are the main novelty of the present work. The experimental data presented in this paper, together with already published data of the Naples Systematic Series, aims at expanding the knowledge base of planing hulls seakeeping.

The first part of the paper deals with the identification of the damping and restoring coefficients associated to different non-linear differential equations that may be adopted to model the experimental free decay. Two approaches have been adopted: a parameter identification technique based on the Levenberg–Marquardt algorithm and the linear decrement of roll decay, the standard procedure recommended by the ITTC for the analysis of roll decay tests.

Results from the application of the Levenberg–Marquardt algorithm have shown that, for hard chine hulls, a differential equation with a cubic non-linear restoring term and a second order damping provides a better fit with respect to a third order damping with linear restoring term (the differential model suggested by the ITTC). Nonetheless, the differences between the two approaches in terms of R^2 are of the order of 10^{-4}. An additional differential model that includes both non-linear damping and restoring is proposed, although it provides a marginally better fit to the data only for two hulls. Concluding, a quadratic damping model is sufficiently accurate to describe damping non-linearity, whereas a cubic restoring term is recommended to properly model the roll dynamics of the warped hard chine hulls tested in this study.

The analysis of the linear decrement of roll decay to characterize the damping coefficients provides results with smaller R^2 values compared to the same parameters obtained via Levenberg–Marquardt algorithm. However, the values are still sufficiently accurate to describe the roll decay.

The damping coefficients obtained with the two different techniques, have been finally used to calculate the equivalent linear roll damping at the reference angle of 5 degrees. The equivalent linear damping coefficients have shown that the most slender model is the one with the highest damping.

Results of regular beam waves on the three models in terms of roll and heave Response Amplitude operators (RAOs) are reported for three models, showing that they share a very similar roll response, in particular for shorter to critical wavelength to model breadth ratios. Heave RAOs show a similar trend with L/B, apart for wavelengths near the critical value where the slender hull shows lower response. In addition, heave-roll phase is plotted for the three hulls showing consistency between the three hulls while slenderness seems to have a negligible effect on phase response.

The hulls have also been tested in irregular beam sea showing that although the average response spectra have a well defined peak, the short time analysis highlights spectral bandwidth modulations, as well as roll beat, characterized by the transition to a bimodal spectra.

Future work will be carried out with the models of the NSS at semi-planing and planing speeds to assess the effect of the hydrodynamic forces on roll damping and restoring coefficients.

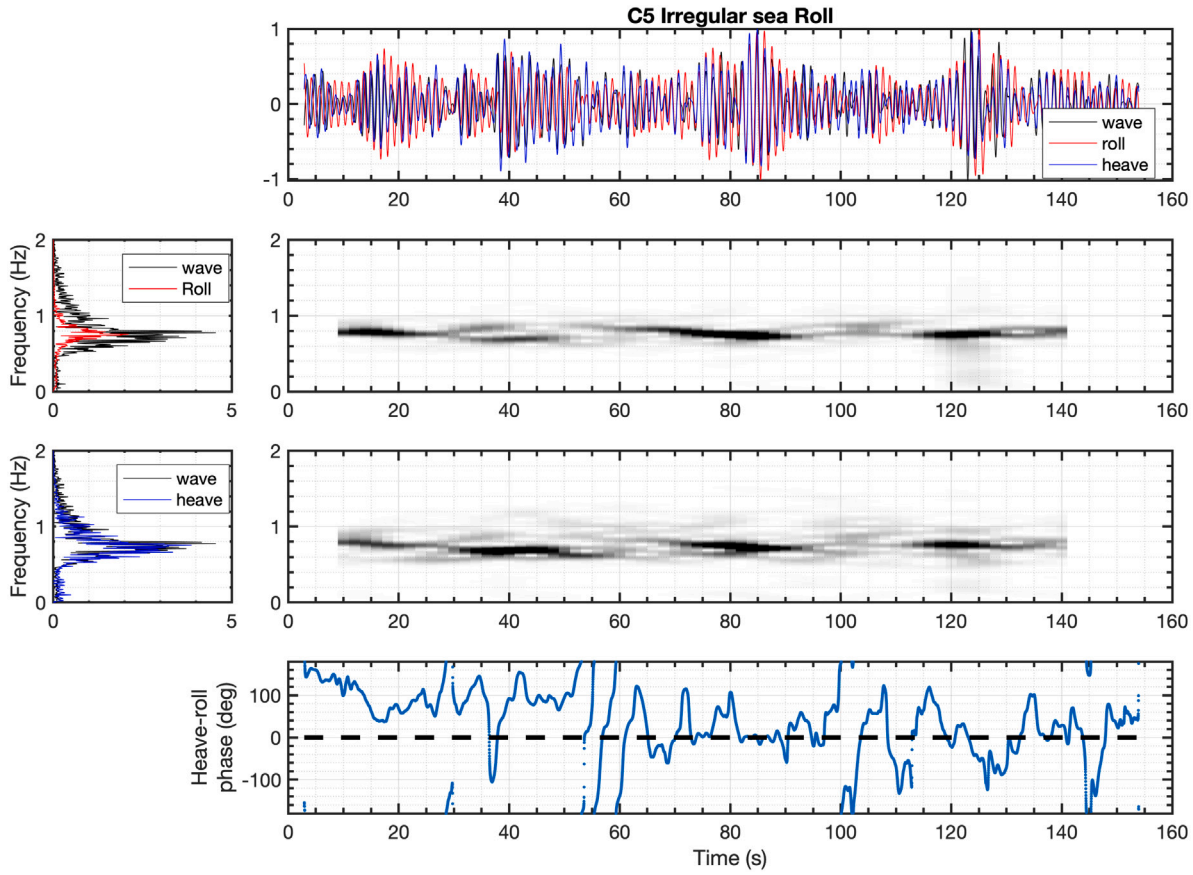

Fig. 8. C5 model irregular waves response.

CRediT authorship contribution statement

Fabio De Luca: Conceptualization, Data curation, Formal analysis, Investigation, Methodology, Software, Writing – original draft, Writing – review & editing. **Riccardo Pigazzini:** Conceptualization, Data curation, Formal analysis, Investigation, Methodology, Software, Writing – original draft, Writing – review & editing. **Gennaro Rosano:** Conceptualization, Data curation, Formal analysis, Investigation, Methodology, Software, Writing – original draft, Writing – review & editing. **Tommaso Coppola:** Funding acquisition, Writing – review & editing.

Declaration of competing interest

The authors declare that they have no known competing financial interests or personal relationships that could have appeared to influence the work reported in this paper.

Data availability

Data will be made available on request.

Acknowledgements

The METROPOLIS project (METodologie RObuste per l'efficientamento dei Processi e l'Ottimizzazione Logistica nell'Industria Siderurgico-navale; Development of innovative approaches for the supply chain optimization and digitalization in the shipbuilding industry), project n. F/190010/02/X44 is acknowledged for its financial support.

References

Balsamo, F., Milanesi, S., Pensa, C., 2001. Rolling dynamic in planing and semi-planing range. In: Proceedings of the 6th International Conference on Fast Sea Transportation. FAST 2001, Southampton, UK.

Begovic, E., Bertorello, C., Pennino, S., 2014. Experimental seakeeping assessment of a warped planing hull model series. Ocean Eng. 83, 1–15.

Begovic, E., Bertorello, C., Pennino, S., Piscopo, V., Scamardella, A., 2016. Statistical analysis of planing hull motions and accelerations in irregular head sea. Ocean Eng. 112, 253–264.

Begovic, E., Bertorello, C., Prpic Orsic, J., 2013. Roll damping coefficients assessment and comparison for round bilge and hard chine hullforms. In: Volume 9: Odd M. Faltinsen Honoring Symposium on Marine Hydrodynamics. American Society of Mechanical Engineers, Nantes, France, http://dx.doi.org/10.1115/OMAE2013-10620, V009T12A024.

Brown, P.W., Klosinski, W.E., 1995a. Experimental Determination of the Added Inertia and Damping of a 30 Degree Deadrise Planing Boat in Roll. Technical Report, Davidson Laboratory Stevens Institute of Technology.

Brown, P.W., Klosinski, W.E., 1995b. Experimental Determination of the Added Inertia and Damping of Planing Boats in Roll. Technical Report, Davidson Laboratory Stevens Institute of Technology.

Bulian, G., Francescutto, A., F., F., 2009. Determination of Relevant Parameters for the Alternative Assessment of Intact Stability Weather Criterion On Experimental Basis, Project HYD-III-CEH-5, Rev.1.0- Final-22, November 2009. Technical Report, DINMA Trieste, www.shipstab.com.

De Luca, F., Pensa, C., 2017. The Naples warped hard chine hulls systematic series. Ocean Eng. 139, 205–236.

De Luca, F., Pensa, C., 2019. The Naples Systematic Series–Second part: Irregular waves, seakeeping in head sea. Ocean Eng. 194, 106620.

Fridsma, G., 1969. A Systematic Study of the Rough-Water Performance of Planing Boats. Technical Report, STEVENS INST OF TECH HOBOKEN NJ DAVIDSON LAB.

Fridsma, G., 1971. A Systematic Study of the Rough-Water Performance of Planing Boats–Part 2 Irregular Waves. Technical Report, Davidson Laboratory, Stevens Institute of Technology, Hoboken, NJ.

Ikeda, Y., Himeno, Y., Tanaka, N., 1978a. A Prediction Method for Ship Roll Damping. Technical Report, Report of Department of Naval Architecture, University of Osaka Prefecture.

Ikeda, Y., Himeno, Y., Tanaka, N., 1978b. Components of Roll Damping of Ship at Forward Speed. Technical Report, Report of Department of Naval Architecture, University of Osaka Prefecture.

Ikeda, Y., Katayama, T., 2000. Roll damping prediction method for a high-speed planing craft. In: Proceedings of the 7th International Conference on Stabilityof Ship and Ocean Vehicles. p. 10.

IMO, 2006. IMO MSC.1/Circ.1200, "Interim Guidelines for Alternative Assessment of the Weather Criterion". Technical Report.

ITTC, 2011. Recommended Procedures - Numerical Estimation of Roll Damping. Technical Report.

Kahramanoglu, E., Yıldız, B., Çakıcı, F., Yilmaz, H., 2021. Numerical roll damping prediction of a planing hull. Ships Offshore Struct. 16 (4), 363–372. http://dx.doi.org/10.1080/17445302.2020.1730088.

Levenberg, K., 1944. A method for the solution of certain non-linear problems in least squares. Quart. Appl. Math. 2 (2), 164–168.

Mancini, S., Begovic, E., Day, A.H., Incecik, A., 2018. Verification and validation of numerical modelling of DTMB 5415 roll decay. Ocean Eng. 162, 209–223. http://dx.doi.org/10.1016/j.oceaneng.2018.05.031.

Marquardt, D.W., 1963. An algorithm for least-squares estimation of nonlinear parameters. J. Soc. Ind. Appl. Math. 11 (2), 431–441.

Pigazzini, R., De Luca, F., Pensa, C., 2021. An experimental assessment of nonlinear effects of vertical motions of Naples systematic series planing hulls in regular waves. Appl. Ocean Res. 111 (September 2020), 102546. http://dx.doi.org/10.1016/j.apor.2021.102546.

Taunton, D., Hudson, D., Shenoi, R., 2011. Characteristics of a series of high speed hard chine planing hulls-part II: performance in waves. Int. J. Small Craft Technol. 153, B1–B22.

Zarnick, E.E., Turner, C., 1981. Rough Water Performance of High Length to Beam Ratio Planing Boats. Technical Report, David W Taylor Naval Ship Research And Development Center Bethesda.